Remote Sensing of Environment 144 (2014) 28–41

Contents lists available at ScienceDirect

Remote Sensing of Environment

journal homepage: www.elsevier.com/locate/rse

Changes in vegetation photosynthetic activity trends across the Asia–Pacific region over the last three decades

Baozhang Chen [a,b,*], Guang Xu [a], Nicholas C. Coops [b], Philippe Ciais [c], John L. Innes [b], Guangyu Wang [b], Ranga B. Myneni [d], Tongli Wang [e], Judi Krzyzanowski [b], Qinglin Li [f], Lin Cao [b], Ying Liu [g,**]

[a] State Key Laboratory of Resources and Environmental Information System, Institute of Geographic Sciences and Natural Resources Research, University of Chinese Academy of Sciences, 11A, Datun Road, Chaoyang District, Beijing, China
[b] Department of Forest Resource Management, University of British Columbia, 2424 Main Mall, Vancouver, BC V6T 1Z4, Canada
[c] Laboratoire des Sciences du Climat et de l'Environnement, Unité Mixte de Recherche Commissariat à l'Energie Atomique-Centre National de la Recherche Scientifique-Université de Versailles Saint-Quentin-en-Yvelines, Batiment 709, CE L'Orme des Merisiers, Gif-sur-Yvette F-91191, France
[d] Department of Earth and Environment, Boston University, 675 Commonwealth Avenue, Boston, MA 02215, USA
[e] Centre for Forest Conservation Genetics, Department of Forest Sciences, University of British Columbia, 2424 Main Mall, Vancouver, BC V6T 1Z4, Canada
[f] Forest Analysis and Inventory Branch, Ministry of Forests, Lands, and Natural Resource Operations, Victoria, BC V8W 9C2, Canada
[g] School of Soil and Water Conservation, Beijng Forestry University, Beijing 100083, China

ARTICLE INFO

Article history:
Received 19 June 2013
Received in revised form 22 December 2013
Accepted 23 December 2013
Available online xxxx

Keywords:
Climate change
Vegetation growth dynamics
NDVI
Time series analysis
Gradual changes
Trend breaks
Breakpoint
Turning point
Asia–Pacific region

ABSTRACT

The updated Global Inventory Modeling and Mapping Studies (GIMMS) third generation global satellite Advanced Very High Resolution Radiometer (AVHRR) Normalized Difference Vegetation Index (NDVI) dataset provides very detailed global information on the state of vegetation from 1982 to 2011. Using these data we investigated the changes in the vegetation photosynthetic activity in the Asia–Pacific (AP) (including Australia, South East Asia, China, and the Pacific Coast of North America) region, by discerning gradual changes into two key metrics: 1) the cumulative annual NDVI in each year and 2) the seasonality or variance in that index. We then assessed changes using break and turning points using three statistical models (least-square linear, expanded paired-consecutive linear and piecewise regression models). We found that the AP region overall experienced increasing NDVI from 1982 through 2011 with an average rate of 5.30×10^{-4} NDVI yr^{-1} (0.13% yr^{-1}). The annual NDVI increased from 1982 at a faster rate of 26.14×10^{-4} NDVI yr^{-1} (0.65% yr^{-1}) until a break in the trend after 1991 (after that the trend reduced to 5.78×10^{-4} NDVI yr^{-1}). In the Asia–Australia (AA) subarea of the AP, vegetation greening slowly increased at 8.71×10^{-4} NDVI yr^{-1} before 2003 and then increased to 28.30×10^{-4} NDVI yr^{-1} after 2003. In contrast, in the North America (NA) subarea NDVI rapidly increased initially at 18.72×10^{-4} NDVI yr^{-1} before 1992 and then marginally increased (3.96×10^{-4} NDVI yr^{-1}) after 1992. The turning points were found to be 2008 and 1987 for the AA and NA subareas respectively. Analysis of monthly NDVI data showed that the trends were positive for most of the months of the study period, particularly during the growing season. Geospatial analyses demonstrated that cumulative annual NDVI and the variance or seasonality across the large AP region varied across the different subareas. As well, we found evidence for different spatial patterns of the NDVI changes with strong spatial heterogeneity in the patterns of the break and turning points. This suggests complex and nonlinear responses of vegetation photosynthetic activity to regional climatic changes and other drivers.

1. Introduction

Vegetation, as the most important component of terrestrial ecosystems, fundamentally regulates the energy budget, water cycle and biogeochemical cycle in the land surface through photosynthesis, respiration, transpiration, surface albedo, and roughness (Jackson, Randerson, Canadell, et al., 2008). Photosynthetic activity affects the Earth climate system and maintains climate stability, through its coupling with transpiration (Anderson, Canadell, Randerson, et al., 2010). Understanding the dynamics of photosynthetic activity and its correlations with climate variability and climate change is one of the important issues of global change research (Nemani et al., 2003). Satellite remote sensing is unique and useful for monitoring vegetation dynamics and environmental changes over large coverage in a repeatable manner (Goward, Tucker, & Dye, 1985; Myneni, Hall, Sellers, & Marshak, 1995; Nemani et al., 2003; Tucker et al., 2001; Zhou et al., 2001).

* Correspondence to: B. Chen, State Key Laboratory of Resources and Environmental Information System, Institute of Geographic Sciences and Natural Resources Research, Chinese Academy of Sciences, 11A, Datun Road, Chaoyang District, Beijing, China. Tel./fax: +86 10 64889574.
** Corresponding author.
E-mail addresses: baozhang.chen@igsnrr.ac.cn (B. Chen), 1191184845@qq.com (Y. Liu).

0034-4257/$ – see front matter © 2014 Elsevier Inc. All rights reserved.
http://dx.doi.org/10.1016/j.rse.2013.12.018

A common way to derive indicators on vegetation and environmental changes is to use spectral vegetation indices (VI). One of the most widely used VI is the Normalized Difference Vegetation Index (NDVI, Rouse, Haas, Schell, & Deering, 1973; Tucker, 1979). The NDVI exploits the contrast in reflectance between the infrared and red portions of the electromagnetic spectrum and has been found to be correlated well with leaf area index (LAI), chlorophyll abundance, absorption of photosynthetically active radiation (fPAR), and gross primary production quantity (GPP) (Goetz & Prince, 1999; Myneni et al., 1995). A number of researchers have used remote sensing imagery to investigate vegetation growth and ecosystem productivity or functioning (e.g. Beck et al., 2011; Box, Holben, & Kalb, 1989; De Jong, Verbesselt, Schaepman, & de Bruin, 2012; Defries & Townshend, 1994; Goetz, Bunn, Fiske, & Houghton, 2005; Miao, Yang, Chen, & Gao, 2012; Park & Sohn, 2010; Peng et al., 2011; Piao, Fang, Zhou, et al., 2003, Piao et al., 2011; Wang et al., 2011; Zhao & Running, 2010) at a wide variety of spatial and temporal scales.

Time series of NDVI data derived from the National Oceanic and Atmospheric Administration's (NOAA) Advanced Very High Resolution Radiometer (AVHRR) meteorological satellites are widely used (Myneni et al., 1995; Nemani et al., 2003; Tucker et al., 2001; Zhou et al., 2001). A number of studies analyzing changes in NDVI found that regional climate trends differentially impacted vegetation dynamics across different ecosystems at various spatial scales (De Jong et al., 2012; Myneni et al., 1995; Nemani et al., 2003; Zhao & Running, 2010).

Trends of increasing vegetation growth, also known as 'greening', have been documented in the Northern Hemisphere (NH) between 35° and 75° latitude (Beck et al., 2011; Slayback, Pinzon, Los, & Tucker, 2003; Zhou et al., 2001) and in few other regions, including the Sahel (Fensholt, Rasmussen, Nielsen, & Mbow, 2009; Olsson, Eklundh, & Ardo, 2005) and parts of Australia (Donohue, Mcvicar, & Roderick, 2009). Nemani et al. (2003) inferred a significant increase of Net Primary Productivity (NPP) from NDVI trends in northern high-latitude ecosystems during the period 1982–1999. By contrast, a decrease of photosynthetic activity over a large part of the boreal forests was found during 1982–2005 (Goetz et al., 2005) and during 1982–2008 (Beck et al., 2011). In addition, it was also found from NDVI observations that the general northern greening in the 1980s and the 1990s (Nemani et al., 2003; Zhou et al., 2001) was weaker in North America (Zhou et al., 2001) than over Eurasia (Piao et al., 2011). Further, De Jong et al. (2012) found that greening trends were weaker in the Southern Hemisphere (SH) than the NH. These findings consistently point out substantially different greening regimes among continents and regions.

The El Niño/Southern Oscillation, Pacific Decadal Oscillation and Arctic Oscillation/North Atlantic Oscillation are known as "natural patterns" of the Earth's climate, which exert important influences on regional climates around the world, especially on the Asia–Pacific (AP) region (including Australia, South East Asia, China, and the Pacific Coast of North America, see Fig. 1) (Catrin & John, 2013; Latif & Barnett, 1994; Newman, Gilbert, & Michael, 2003; Patterson, Chang, Prokoph, Roe, & Swindles, 2013), characterizing signatures in seasonally changing patterns of wind, air temperature, and precipitation. The AP region experienced faster environmental changes than the global average during the last few decades and will likely experience more climate extreme events and phenomena (Cruz, Harasawa, Lal, et al., 2007; Hansen, Ruedy, Sato, & Lo, 2010; USAID, 2010; Yao, Yang, Qian, Lin, & Wen, 2008). This region and its ecosystems are particularly vulnerable to climate changes (Preston, Suppiah, Macadam, & Bathols, 2006). The AP region also encompasses both developed and developing nations. This justifies a comparative investigation of changes in NDVI between the western (Asia–Australia (AA)) and the eastern part (North America (NA)) of the AP region. Considering the climatic uniqueness and importance of the AP region, we choose the AP region as the object of this study.

Most of the previous studies only used seasonal or annual mean NDVI, an indicator of cumulative annual vegetation productivity. The standard deviation of NDVI over a year which provides an indication of the seasonality or variance of the photosynthetic activity is another remote sensing indicator to capture vegetation dynamics. This study expands the NDVI time series analysis by including the annual s.d. indicator to assess changes in vegetation dynamics and to answer the question: how does NDVI seasonality change and is it consistent with the change of cumulative annual mean NDVI in the AP region?

Changes in vegetation dynamics can be characterized by seasonal changes, gradual trend changes and abrupt changes (De Jong et al., 2012). The gradual changes refer to the trend component beyond the seasonal variation, slowly acting environmental processes (De Jong et al., 2012). Over time, these gradual changes in vegetation photosynthetic activity during the 1980s and 1990s may stall or reverse (Angert, Biraud, Bonfils, et al., 2005; Lotsch, Friedl, Anderson, & Tucker, 2005; Park & Sohn, 2010; Scheffer, Carpenter, Foley, Folke, & Walker, 2001; Wang et al., 2011; Zhao & Running, 2010; Zhao & Running, 2010). Most of these studies used time series of NDVI data from 1982 to 2006 or shorter. For example, De Jong et al. (2012) used NDVI data updated to 2008 and Wang et al. (2011) extended the study period to 2010 however only for China. In this study, we extended the study period until 2011 to analyze trend changes in vegetation photosynthetic activity using a 30-year long time series of NDVI data in the AP region. With the longest available NDVI series data, this study intends to answer the following three questions:

- How did the direction and rate of NDVI trend change temporally and spatially during the past 30-year period across the AP region?
- Are the previously observed trends in vegetation NDVI consistent with the trends during the last decade? For instance a reversal in the trend of vegetation NDVI in the late 1990s was found in Eurasia (Piao et al., 2011) and in the late 1980s/early 1990s in North America (Wang et al., 2011)?
- Is the global result that weaker greening in the SH while stronger greening in the NH (De Jong et al., 2012) applicable to the AP region?

To answer these questions, we analyzed changes in annual, growing season and monthly mean NDVI, and its annual standard deviation (s.d.) at a resolution of 8 km for the AA and NA regions.

2. Research area and dataset

2.1. Research area

We selected the AP as our research area (Fig. 1), which contains two subareas: the AA subarea (48°S–54°N, 73°–180°E) and the NA subarea (30°–72°N, 100°–168°W). The former covers much of East Asia, Southeast Asia and Australia, and the latter covers Alaska, Western Canada and Northwest USA. The AP contains almost all forest types on Earth, including tropical, sub-tropical, temperate and boreal forests, montane forests, and mangrove forests. The AP is predicted to be particularly vulnerable to climate change outcomes when compared to the rest of the world (Cruz et al., 2007; Hansen et al., 2010; USAID, 2010; Yao et al., 2008).

2.2. Dataset

In this study we used the Global Inventory Modeling and Mapping Studies (GIMMS) third generation NDVI dataset derived from the AVHRR sensors (NDVI3g) at a spatial resolution of 1/12° and 15-day interval, spanning from July 1981 to December 2011 (Myneni, Keeling, Tucker, Asrar, & Nemani, 1997; Tucker et al., 2005). This reanalysis improved AVHRR data quality in the northern parts of the world by using improved calibration procedures and calibrated using Sea-viewing Wide Field-of-view Sensor (SeaWiFS) data (Høgda et al., 2013). The GIMMS NDVI dataset has been corrected to minimize various deleterious effects, such as calibration loss, orbital drift and volcanic eruptions, and has been verified using stable desert control points (De Jong, Verbesselt, Zeileis, & Schaepman, 2013; Tucker et al., 2005; Xu et al., 2013; Zeng, Collatz, Pinzon, & Ivanoff, 2013).

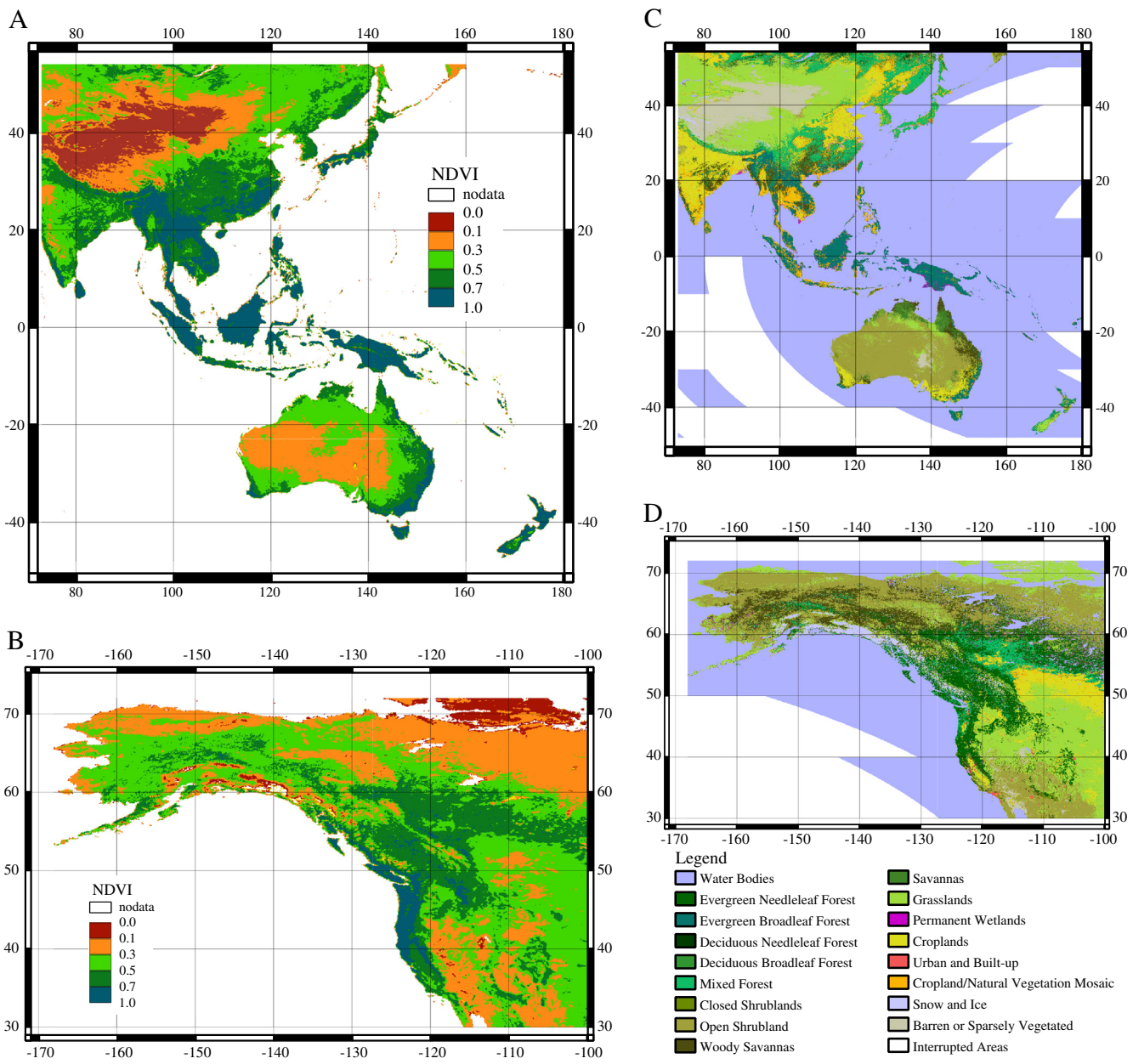

Fig. 1. Geographical distribution of the 30-year (1982–2011) mean NDVI (A, B) and land cover (C, D) over the two large subareas in the AP region: the Asia–Australia (A, C) and the North America (B, D) regions. The land cover maps (C, D) were obtained from Moderate Resolution Imaging Spectrometer (MODIS) land cover dataset (MOD12Q1 product for the year 2011), acquired from http://edcimswww.cr.usgs.gov/pub/imswelcome. The MODIS land cover dataset consists of 17 general land cover types based on the International Geosphere and Biosphere Programme (IGBP) LC classification scheme.

The GIMMS NDVI3g series is the only continuous and up-to-date global NDVI dataset that is continually assessed and validated (Beck et al., 2011). Globally, trends in the GIMMS NDVI3g compare favorably with trends derived from Landsat (Beck et al., 2011) and Moderate Resolution Imaging Spectrometer (MODIS) NDVI (Fensholt & Proud, 2012; Zeng et al., 2013). Fensholt and Proud (2012) evaluated the accuracy of the GIMMS NDVI3g by comparison with the global Terra MODIS NDVI (MOD13C2 Collection 5) data using linear regression trend analysis and the regression coefficient (slope value) ($P < 0.01$) was found to be close to 1 for most land cover types on a global scale (Fensholt & Proud, 2012). Zeng et al. (2013) reported that the trends of GIMMS NDVI were in overall acceptable agreement with MODIS NDVI data. These comparisons build confidence that the 30-year GIMMS AVHRR NDVI3g record thus provides a robust time series to explore changes in vegetation photosynthetic activity as expressed by NDVI (Fensholt & Proud, 2012; Zeng et al., 2013).

3. Methods and analysis

3.1. Data selection and pre-analysis

We excluded the half year of 1981 and used exactly thirty years of data composed of 720 fortnightly observations in our analysis. AVHRR observations are often affected from snow or cloud cover, which values are flagged as “snow” or “clouds” in the GIMMS NDVI3g dataset (Xu et al., 2013). These “flagged” data were excluded from the analysis and the gaps were interpolated to keep the 15-day interval time series being consecutive (24 data points a year). To exclude potentially

remaining effects of cloud or haze contaminations or other noises, the dataset was further aggregated to monthly temporal resolution using the maximum value following the method of Congalton (1991). Pixels with a 30-year averaged NDVI value of less than 0.1 were classified as non-vegetated area and were masked out following the method of Piao et al. (2011). We then calculated the annual mean (μ) and annual standard deviation (σ) from the monthly composite NDVI values for each year from 1982 to 2011 for each vegetated pixel. The following analysis was conducted on either the yearly (annual μ and σ) or monthly (each calendar month's value) time basis and the total data points of the NDVI time series in this study, $N = 30$. The gradual change trend, breakpoint (BP) and turning point (TP) were estimated using the following three models (see Section 3). For deriving trends for individual segments the slopes of the trend were estimated by linear least-squares regression of the annual or monthly (each calendar month's value) against time. Following the method of Mann (1945), we estimated the significance of the trend in each time series segment by applying the Mann–Kendall trend test.

All the above data analyses were implemented at both pixel and regional scales. At the regional scale, we respectively aggregated all the pixel values for each month or annual to respectively form one time series for the AP, AA and NA regions first, and then we estimated the regional trend, variance, BP, and TP based on these time series NDVI data.

3.2. Detecting a gradual change at a constant rate (trend, Model 1)

To detect gradual change of the NDVI time-series during the 30-year period, a least-square linear regression model (Piao et al., 2011) was applied,

$$y_t = a + bx_t + \varepsilon : \quad x_t \in \{1 \ldots N\} \tag{1}$$

where y_t represents the NDVI time-series, x_t is the time (year or calendar month), a and b are the regression parameters (a is the intercept and b is the trend (slope)), and ε is the residual of the fit.

3.3. Detecting breakpoints in time series (BP, Model 2)

A gradual change over a time series of NDVI values may stall or reverse. Such an event when there is a significant change in slope is defined as an abrupt change (Verbesselt, Hyndman, Newnham, & Culvenor, 2010) with a breakpoint (BP), in other words, the BP breaks down the time series into two independent segments with a significant change in slope. Given a time series $x_t = 1,2,3 \ldots N$, the time series is broken down into two consecutive segments by a moving point k, $k \in 3 + i$, $i = 1,2,\ldots N - 3$ with a moving step $i = 1$. A least-square linear regression model (Eq. 1) is applied to each of the paired time series segments,

$$\begin{cases} y_t = a_{bk} + b_{bk}x_t + \varepsilon & x_t \le k, \qquad |k \in 3 + i, \{i = 1, 2, \ldots N-3\} \\ y_t = a_{ak} + b_{ak}x_t + \varepsilon, & k \in 3 + i, \{i = 1, 2, \ldots N-3\} \end{cases} \tag{2}$$

where y_t is the NDVI time-series (i.e. annual μ or σ or calendar month's values), x_t is the time (year or calendar month), k is the time point breaking down the NDVI time-series into two paired consecutive segments and which are independent from each other, a and b are the fitted intercept and trend (slope), respectively; the subscripts $_{bk}$ and $_{ak}$ refer the regression parameters for the two paired segments before and after k, respectively; and ε is the residual of the fit. An F-test was used to detect the significance of slopes (b_{bk} and b_{ak}) of both paired segments before and after k against the null hypothesis that the slope $b = 0$ at $\alpha = 0.05$ (degrees of freedom equals the number of observations in the segment minus 2). To avoid error coming from too short segments we only consider segment of the time series with data points larger than 4 among a total of 30 data points. Only if (i) both b_{bk} and b_{ak} are significant, and (ii) the former is significantly different from the latter ($P < 0.05$), the point in time $x_t = k$ is considered as the BP. Otherwise we consider that no BP occurred over the 30-year NDVI time series. This procedure is similar to the ordinary-least squares moving sum test for the existence of breakpoints in the time series. If the test indicates more than one BPs exist, to simplify the analysis in this study, we only select the one BP with the highest overall significance level. This major BP is estimated by minimizing the Bayesian Information Criterion (BIC), i.e. by minimizing the residual sum of squares of this regression for both segments (Bai & Perron, 2003; Zeileis, Kleiber, Krämer, & Hornik, 2003).

3.4. Detecting turning point (TP, Model 3)

We used a piecewise regression approach with one TP (Toms & Lesperance, 2003) to examine if there is a TP during the study period,

$$y_t = \begin{cases} a_0 + b_1x_t + \varepsilon, & x_t \le j, \quad j \in \{4, 6, \ldots N-4\} \\ a_0 + b_1x_t + b_2(x_t - j) + \varepsilon, & x_t > j \end{cases} \tag{3}$$

where y_t is the NDVI time-series (i.e. annual μ or σ or calendar month's values), x_t is the time (year or calendar month); j is the TP of the NDVI time-series, α_0, b_1 and b_2 are the regression coefficients; α_0 is the fitted intercept, and ε is the residual of the fit. The NDVI trend is b_1 before the TP, and $b_1 + b_2$ after it. We also require that $\alpha \in \{4,6,\ldots N-4\}$ to eliminate two consecutive segments before and after j with too few data points. It is worth noting that a TP is different from a BP in that the former does not break down the whole consecutive change over the entire study period into two independent segments while the latter does. The slope before a TP is significantly different from the slope following however the two segments before and after share the same slope b_1 (see Eq. 3, this also can be seen in Fig. 2 for instance, the trend lines before and after a TP are connected, but the trend lines before and after a BP are disconnected). This model has been widely applied in previous studies (Francesco Ficetola & Denoël, 2009; Peng, Liu, Liu, Wu, & Han, 2012; PIAO et al., 2011; Sun et al., 2011; Swift & Hannon, 2010; Wang, Wang, Piao, & Fang, 2010; Wang et al., 2011). The TP is determined by the maximum likelihood (least-square error) method. If the null hypothesis of $b_2 = 0$ is rejected, change in trends before and after the TP is significant because b_2 is the difference between the trend before and after the turning point.

3.5. Evaluation of the fit models

A F-test was used to assess each model's statistical significance. The linear slope of each model was analyzed against the null hypothesis that slope $b = 0$ at $\alpha = 0.05$ (degrees of freedom equals the number of observations in the segment minus 2). A P value 0.05 was considered significant.

We compared the three models (Eqs. 1, 2, and 3) and evaluated the BP and TP using the Akaike information criterion (AIC) method,

$$\lambda = n \ \log\left(\frac{E}{n}\right) + 2k + \frac{2k(k+1)}{n-k-1} \tag{4}$$

where λ is the AIC value, E is the residual sum of squares for the estimated model, n is the sample size and k is the number of parameters in the model. The difference in AIC values between models j and i (i.e., λ_j and λ_i, respectively), $\Delta\lambda_{j,i} = \lambda_j - \lambda_i$, can be used to assess which fitting model performs the best. Following the rule of thumb of Burnham and Anderson (2002), a threshold of $\Delta\lambda_{j,i} = 2$ is considered to be a critical value for model i to be preferred over the alternative model j; otherwise if $|\Delta\lambda_{j,i}| < 2$, the difference in fitting performance between these two models is not significant.

We evaluated the performances of Model 2 and Model 3 against Model 1 by calculating $\Delta\lambda_{2,1}$ and $\Delta\lambda_{3,1}$. Through this analysis, we determined which of these three regression models (Eqs. 1, 2, and 3) preferentially fit the time series of NDVI data whether either the BP or TP is significant.

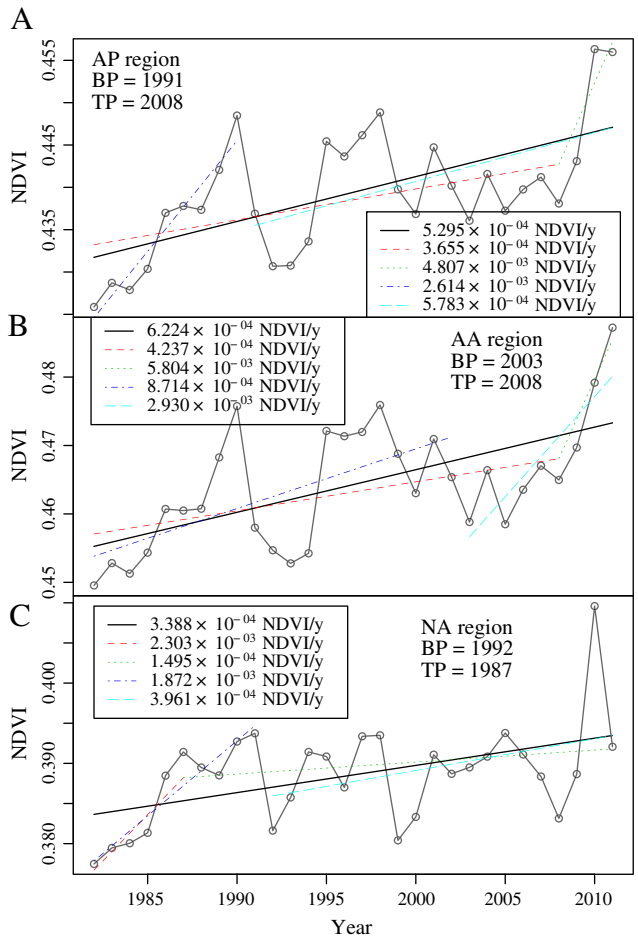

Fig. 2. Interannual variations of annual mean NDVI from 1982 to 2011 for the entire Asia–Pacific (AP) region (A), and sub-regions: the Asia–Australia (AA) region (B) and the North America (NA) region (C).

4. Results

4.1. The 30-year mean NDVI

The spatial distribution of the 30-year mean NDVI (Fig. 1) shows that the non-vegetated area (NDVI < 0.1) accounts for about 8% of the total AP area (~4.3×10^9 ha) (Table 1), mainly occurring in Asia and Australia. Surrounding those regions are open shrub lands, grasslands, and savannas with NDVI values in the range of ~0.2–0.6. High NDVI values (>0.7) are mostly in forests, in the Pacific coastal regions south of 58°N, and the south Asia islands and over the eastern coastal of Australia.

4.2. Changes in vegetation photosynthetic activity dynamics at the continental scale

Fig. 2 and Table 2 show the interannual variation of annual mean NDVI in the entire AP region and the subareas AA and NA from 1982 to 2011. The AP and its component subareas (AA and NA) show an increasing trend. A statistically significant and positive linear trend was estimated using Model 1 (Eq. 1). The trends values are of 5.30, 6.22 and 3.39×10^{-4} NDVI yr^{-1} for AP, AA and NA, respectively ($P < 0.01$) during the 1982–2011 period. Table 2 also shows that the regional average vegetation NDVI over the last three decades is greater in AA than in NA (6.23 versus 3.38×10^{-4} NDVI yr^{-1}).

The BP detected by Model 2 (Eq. 2) based on the 30-year time-series data was 1991, 2003 and 1992 for the AP area and AA and NA subareas, respectively. For the AA subarea, the annual NDVI increased at a rate of 8.71×10^{-4} NDVI yr^{-1} before 2003, but this increase strongly accelerated (28.30×10^{-4} NDVI yr^{-1}) after 2003 (Fig. 2B). By contrast, for the NA subarea, the annual NDVI rapidly increased at a rate of 18.72×10^{-4} NDVI yr^{-1} from 1982 to 1992 (the BP year) and then slowed down to 3.96×10^{-4} NDVI yr^{-1} during 1992–2011 (Fig. 2B). When the whole AP region was considered, the increasing rate of annual NDVI during 1982–1991 was found to be much larger than after 1991 (the BP year) (26.14 versus 5.78×10^{-4} NDVI yr^{-1}). It seems that the AA dominated the whole AP because the area of AA is about two times of NA (Table 1).

Model 3 predicted TP years 2008, 1987 and 2008 for the entire AP region, and subareas NA and AA, respectively (Fig. 2 and Table 2). The AIC of Model 3 is smaller than that of Model 1 by a factor 2 ($\Delta\lambda_{3,1} < -2$, Table 2), indicating an improved likelihood in the piecewise regression model with more parameters despite its increased complexity in comparison to a simple linear regression model. In the AA region the vegetation greening rate was an order of magnitude larger after 2008 (TP) than before (58.04 versus 4.23×10^{-4} NDVI yr^{-1}). In the NA subregion, the annual productivity increased quickly from 1982 to 1987 and then remained nearly flat after the TP (23.03 versus 1.50×10^{-4} NDVI yr^{-1}). However, neither of the trends before and after the TP is statistically significant. Contrast to the fit from Model 3, all the trends detected by Model 1 and Model 2 for the three regions are significant (Table 2). This suggests that Models 1 and 2 are more robust models to fit the 30-year series of NDVI observations. We also compared the trends using annual mean NDVI vs. growing season mean values and found that the identified trends and changes in trends are similar.

The trend in annual or growing season NDVI is an average of trends in each month. To detect more detailed changing signals at finer temporal scales, we conducted the same analysis at monthly scales. The regression results calculated using the three models are shown in Table 3. The trends calculated by the three approaches (Eqs. 1–3) are positive for most months, particularly the growing season months. In the AP and AA regions, monthly NDVI persistently and gradually increased from 1982 through 2011 from March through to November ($P < 0.05$) at a rate of $3.76–11.91 \times 10^{-4}$ NDVI yr^{-1}. By contrast, in the NA, NDVI significantly increased in July, August, September and November, but in the spring months (February to May) NDVI marginally decreased at a rate of -0.13 to -2.24×10^{-4} NDVI yr^{-1} ($P > 0.05$). The detected significant BPs and TPs vary from month to month. The trends before and after BP are statistically significant for most of months over the entire AP, but this is rarely the case for the TP. However, NDVI changes in most of the growing season months (May through September for AP, June through September for AA and March to August for NA) are better described with Model 3 than Model 1.

4.3. Spatial patterns of changes in vegetation photosynthetic activity dynamics

4.3.1. The AA subregion

Fig. 3 shows the geographical distribution of NDVI trends (annual mean and s.d.) and covariation between them during the period 1982–2011 over the AA subregion. About half of the region show insignificant changes in both annual NDVI (57%) and s.d. (54%) (Table 4). The increase of annual NDVI is significant over 27.7% of the AA subregion, particularly over India, southern and southeastern China, Burma,

Table 1
The areas ($\times 10^9$ ha ($\times 10^5$ pixels)) and the proportions of vegetated area over the Asia–Australia (AA), North America (NA) and the whole Asia–Pacific study regions.

Region	Total area $\times 10^9$ ha ($\times 10^5$ pixels)	Vegetated (%)
AP	4.3 (6.7)	91.8
AA	2.9 (4.6)	90.2
NA	1.4 (2.1)	95.4

Table 2
Statistical parameters of the regression models (Eqs. 1–3) against the 30-year series of annual mean NDVI data for the Asia–Australia (AA), North America (NA) and the whole Asia–Pacific (AP) study regions. Trends are in 1×10^{-4} yr^{-1}. $\Delta\lambda_{3,1}$ is the difference of the Akaike information criterion (AIC) values (Eq. 4) between the piecewise regression model (Eq. 3) and the simple linear regression model (Eq. 1).

Region	Model 1		Model 2			Model 3		
	Overall trend	BP	Trend before BP	Trend after BP	TP	Trend before TP	Trend after TP	$\Delta\lambda_{3,1}$
AP	5.30*	1991	26.14*	5.78*	2008	3.65	48.07	−3.40
AA	6.22*	2003	8.71*	29.30*	2008	4.23	58.04	−3.13
NA	3.39*	1992	18.72*	3.96*	1987	23.03	1.50	−2.27

* Indicates significant level ($P < 0.05$).

Malaysia, Indonesia, Philippines, Taiwan, and central and southern Japan where the magnitude of the annual mean NDVI trend exceeds 0.002 yr^{-1} (Fig. 3A).

By contrast, only about 5% of the AA subarea present a significant decreasing trend in annual NDVI. Regions where this decrease is most pronounced (annual mean NDVI < -0.001 yr^{-1}) are northeastern China, eastern Mongolia and southern Russia. It is worth noting that within the area of significant increases in annual NDVI (southeastern China), smaller subareas exhibit a sharp decline (< -0.0015 yr^{-1}, in the Yangtze River and Pearl River deltas) likely because of rapid urban expansion.

About one third of the AA region show a significant increase trend in of NDVI variance (s.d.). These pixels are mainly located in southwestern Russia, Kazakhstan, India, northeastern and eastern China, Sichuan basin of China, and northeastern Australia (where the magnitude of the trend of s.d. of NDVI exceeds 0.001 yr^{-1}) (Fig. 3B).

The covariation between the significant decrease in annual NDVI and the significant increase in annual NDVI variance or seasonality presents in boreal area, such as northeastern China, eastern Mongolia and southern Russia (Fig. 3C), which accounts for about one third of the significant covariance area (Fig. 3D). In most area of India and Burma, both annual mean and variance of NDVI increase (cyan color in Fig. 3C, D), this may be a consequence of changes in Indian monsoon induced by global warming. Whereas, in most of subtropical and tropical regions, a significant increase in annual NDVI covary with insignificant changes or decreasing trends in s.d. of NDVI (e.g. southern China, Malaysia,

Table 3
Statistical parameters of the regression models (Eqs. 1–3) against the 30-year series of monthly mean NDVI data from 1982 to 2011 over the entire Asia–Pacific (AP) study regions and two large sub-regions: the Asia–Australia (AA) and North America (NA). Trends are in 1×10^{-4} yr^{-1}.

Month	Overall trend	BP	Trend before BP	Trend after BP	TP	Trend before TP	Trend after TP
AP							
Jan	1.81	2003	6.56*	16.66*	1988**	22.25	−0.98
Feb	2.93	1986**	−68.40	−0.56	1988	22.55	0.26
Mar	3.76*	1986	−35.41	1.32	1997	9.41	−2.48
Apr	7.26*	1997	6.80	−5.07	1998	12.94	−0.42
May	5.78*	1999**	21.32*	9.55	1990**	31.69*	−0.49
Jun	5.22*	1992	36.93*	6.44	1988**	32.41	1.52
Jul	7.37*	2009**	3.659	134.54	2008**	3.46	109.30*
Aug	8.27*	2009**	3.92	108.42	2008**	4.00	119.56*
Sep	7.64*	1991	39.00*	11.17*	2008**	4.69	83.49
Oct	9.49*	1999	14.43*	31.20*	2008	6.70	82.36
Nov	5.32*	1991	24.04	8.51*	1985	37.57	4.09
Dec	−1.08	1991	14.40	0.52	1985	25.76	−2.10
AA							
Jan	2.52	2003	10.46*	21.36*	1988**	32.69	−1.59
Feb	4.44	1986**	−102.75	0.13	1988	27.87	1.24
Mar	6.63*	2005	10.21*	42.14*	1997	12.33	0.33
Apr	11.91*	1997	7.64	0.001	2008	10.56	47.03
May	9.14*	2003	15.04*	44.04*	2008	6.64	74.39
Jun	4.67*	2003	8.39*	37.51*	2008**	1.71	81.76
Jul	6.01*	2009	2.54	181.75*	2008**	1.98	111.28
Aug	8.54*	2009	3.81	104.03	2008**	3.99	127.07*
Sep	8.99*	2000	12.46*	33.87*	2008**	5.28	105.97
Oct	9.53*	1999	17.60*	38.00*	2008	6.51	88.34
Nov	4.76*	1991	32.54*	6.37	1985	61.64	2.57
Dec	−2.21	2002	4.02	3.75	1985	45.32	−4.03
NA							
Jan	0.35	2009	−0.91	−26.96	2004	−1.36	9.65
Feb	−0.13	1985	−33.47	−1.67	1986	23.05	−1.61
Mar	−2.11	1986	17.87	−5.69*	1986**	46.28	−5.20
Apr	−2.24	2008	3.33	20.62	2005**	3.64	−45.41
May	−1.09	1999	30.15*	7.85	1991**	43.73*	−15.01
Jun	6.36	1999	21.31*	35.61*	1988	43.88	1.25
Jul	10.16*	2009**	5.97*	37.98	2007**	5.80	78.23
Aug	7.74*	2006	3.90	71.74*	2008**	4.04	104.21*
Sep	4.76	1990	47.50*	4.22	1986	55.75	1.50
Oct	9.42*	2007	8.54*	83.77	2008	7.09	70.12
Nov	6.38*	2009**	2.60	−64.42	2006**	2.45	47.23
Dec	1.23	2009	−0.23	−77.03	1995	−3.64	4.83

* Indicates significant level ($P < 0.05$).
** Indicates significant turning point in terms of AIC.

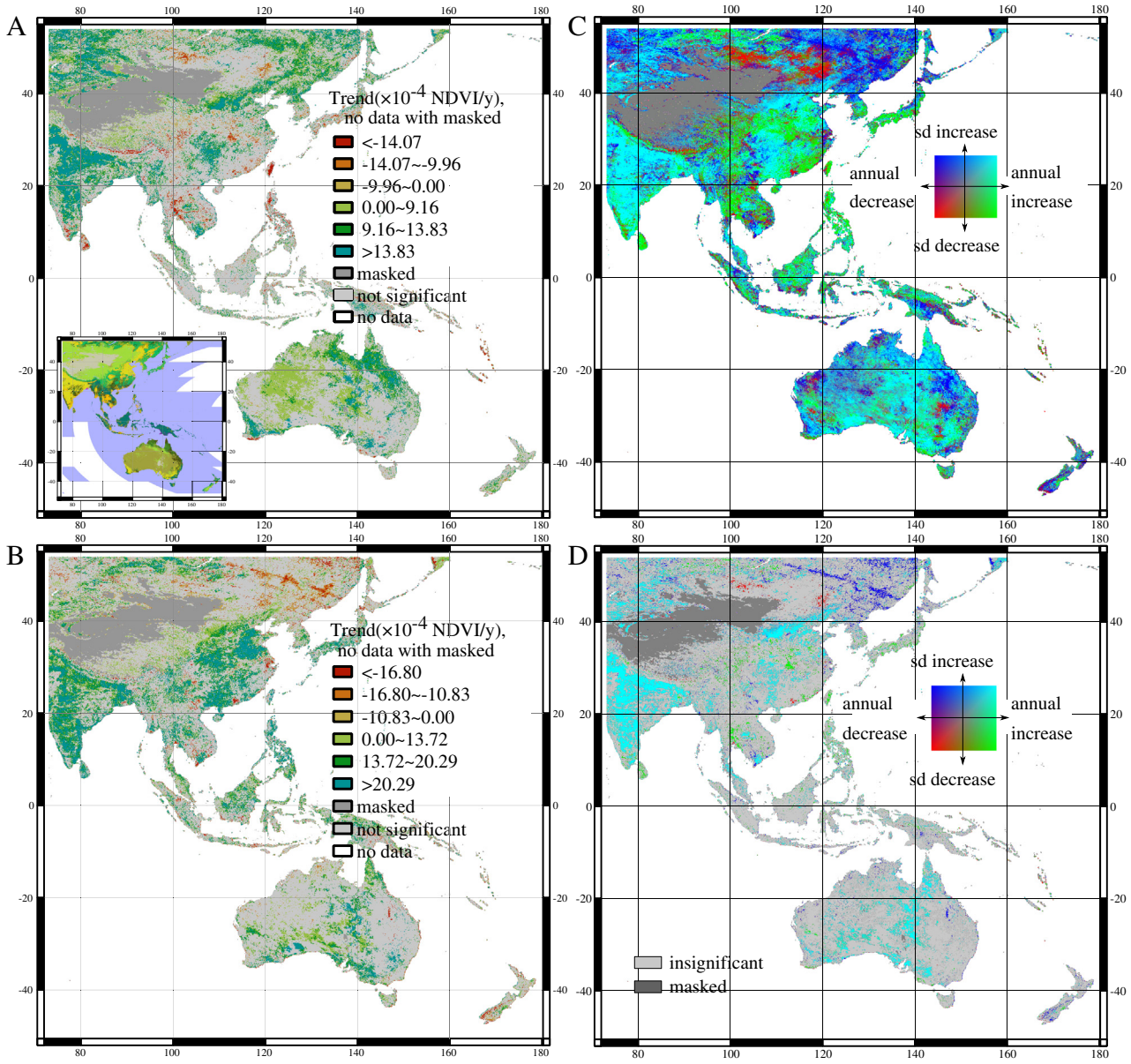

Fig. 3. Spatial distribution of vegetation dynamic changes in the Asia–Australia (AA) region from 1982 to 2011: trend of annual photosynthetic activity (annual mean NDVI trend) (A), trend of photosynthetic activity seasonality (annual s.d. of NDVI) (B), and covariance between annual mean and s.d. trends (C and D). For legend of the inset land cover map in panel (A) see Fig. 1.

Indonesia, Philippines, Taiwan, and Japan) (Fig. 3C, D), suggesting that the annual increase is then driven by an increase of minimum values.

4.3.2. The NA subregion

Fig. 4 shows the spatial distribution of trends in NDVI during the period 1982–2011 over the NA subregion. Across this entire subregion, 49% and 47% of the grid cells show statistically significant changes in annual NDVI and s.d. of NDVI, respectively (Table 4). Of these cells, 73% (36% of total) and 78% (36% of total) display positive NDVI trends for annual NDVI and s.d. of NDVI, respectively, and the remainder display negative trends.

Sub-regions within NA where vegetation experienced a fast increase in both NDVI and in the s.d. of NDVI (slope >0.0015 NDVI yr^{-1}) are mainly in the high latitudes (north of 65°N, e.g. northern Alaska,

Table 4
Statistical summary of vegetation dynamics (% of total area) from 1982 to 2011 over the entire Asia–Pacific (AP) study region and two subareas: Asia–Australia (AA) and North America (NA) regions.*

Regions	Non-vegetated	Annual photosynthetic activity (annual mean NDVI)			Seasonality (annual standard deviation of NDVI)		
		Insignificant trend	Significantly greening	Significantly browning	Insignificant trend	Significantly increasing	Significant decreasing
AA	10.90	56.8	27.75	5.63	54.25	31.89	4.03
NA	4.77	46.16	35.78	13.50	48.63	36.48	10.34
AP	8.89	53.44	30.29	8.12	52.47	33.34	6.02

* A *P* value <5% was considered significant.

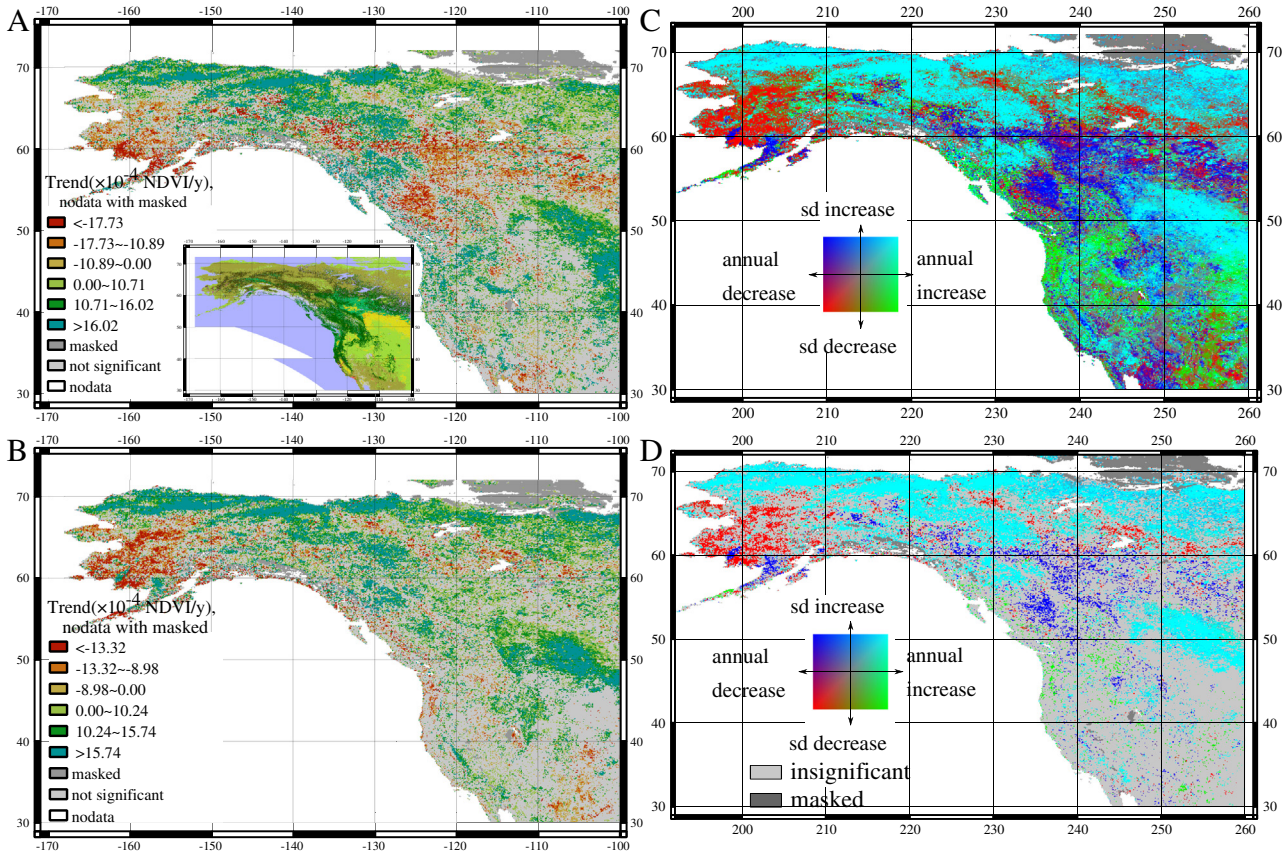

Fig. 4. Same as Fig. 3 but for the North America (NA) region.

Yukon Territory, North West Territory) and in a sub-region bounded by (54°–40°N and 110°–100°W, e.g. western Montana, North Dakota, South Dakota and Nebraska) (Fig. 4C, D). The highest positive trends of NDVI occur in tundra, temperate grasslands and croplands. Sub-regions of NA where NDVI significantly decreased at a fast rate (trend < -0.0015 NDVI yr^{-1}) are in southern Alaska and north east British Columbia–Alberta–Saskatchewan. These regions are covered by boreal forests or grasslands. The transition from positive to negative significant NDVI slopes occurred at the boundary between tundra, crop, grasslands and forests (Fig. 3A). A large decline of NDVI s.d. (rate < -0.001 NDVI yr^{-1}) was only found in southern Alaska where annual NDVI also significantly decreased (Fig. 4C, D), suggesting a decrease in both annual maximum and minimum NDVI during the past 30 years. Even though vegetation experienced browning in British Columbia–Alberta–Saskatchewan, the s.d. of NDVI continued to increase in this area from 1982 to 2011 (Fig. 4C, D). This phenomenon was also found in boreal Asia (Fig. 3C, D), suggesting a decrease in annual minimum or an increase in annual maximum NDVI and meanwhile a decline in annual accumulative NDVI, which may be caused by warming and warming-induced drought in boreal area.

The whole study subregion (~4.3×10^9 ha, 6.71×10^5 pixels) is about 92% vegetated, of which about 42% was found to have statistically significant changing trends in annual mean NDVI (~80% increasing and 20% decreasing) over the past 30 years. The average greening and browning rates were about 1.8×10^{-3} yr^{-1} and -1.7×10^{-3} yr^{-1}, respectively.

4.3.3. BP and TP of annual NDVI trend

Figs. 5 and 6 show spatial distribution of the BP and TP of annual NDVI trend and the trends before and after the BP and TP in AA and NA regions, respectively. Table 5 shows the areas of pixels with statistically significant BPs and TPs of annual NDVI during the period of 1982–2011 over the AP region and its two components (AA and NA). The AIC method determines significant BP and TP values during the period of 1982–2011 over 26% and 49% of the whole AP region, respectively. Area of significant BP is much smaller than that of TP for both AA (23% vs. 46%) and NA (33% vs. 57%) subregions (Table 5, Figs. 5 and 6).

In general, the determined BPs and TPs of annual mean NDVI trend occurred from the 1980s through the middle of the 2000s and varied markedly from region to region although previous studies generally arbitrarily set the same break year of NDVI time series for all regions (e.g. Angert et al., 2005; Tucker et al., 2001). The spatial distributions of BP and TP are highly heterogeneous except for Australia, where both BPs and TPs of annual NDVI occurred during the 2003–2008 period, especially in the central, eastern and southern Australia. In the central area of Northern Territory of Australia, the TP appeared in the 1980s or early 1990s (Fig. 5A, D). Of the significant BPs and TPs in Asia, about 30% and 15% occurred after 2000 and concentrated in the region of Guansu–Ningxia–Shanxi–Hubei–Jiangxi provinces; whereas the remainder (occurring before 2000) distributed across the entire study area in Asia and about half of which occurred in 1980s and half of which occurred in 1990s (Fig. 5A, D). In northeastern China, eastern Mongolia and southern Russia, the BPs and TPs occurred after and

Fig. 5. Geographic distributions of the breakpoint year (BP determined using Model 2, panel A), turning point year (TP determined using Model 3, panel D) of annual mean NDVI trend in the Asia–Australia region during the period of 1982–2011 and the trends of annual mean NDVI before and after the BP (panels (B) and (C), respectively) and TP (panels (E) and (F), respectively) are also shown. For legend of the inset land cover map in panel (A) see Fig. 1.

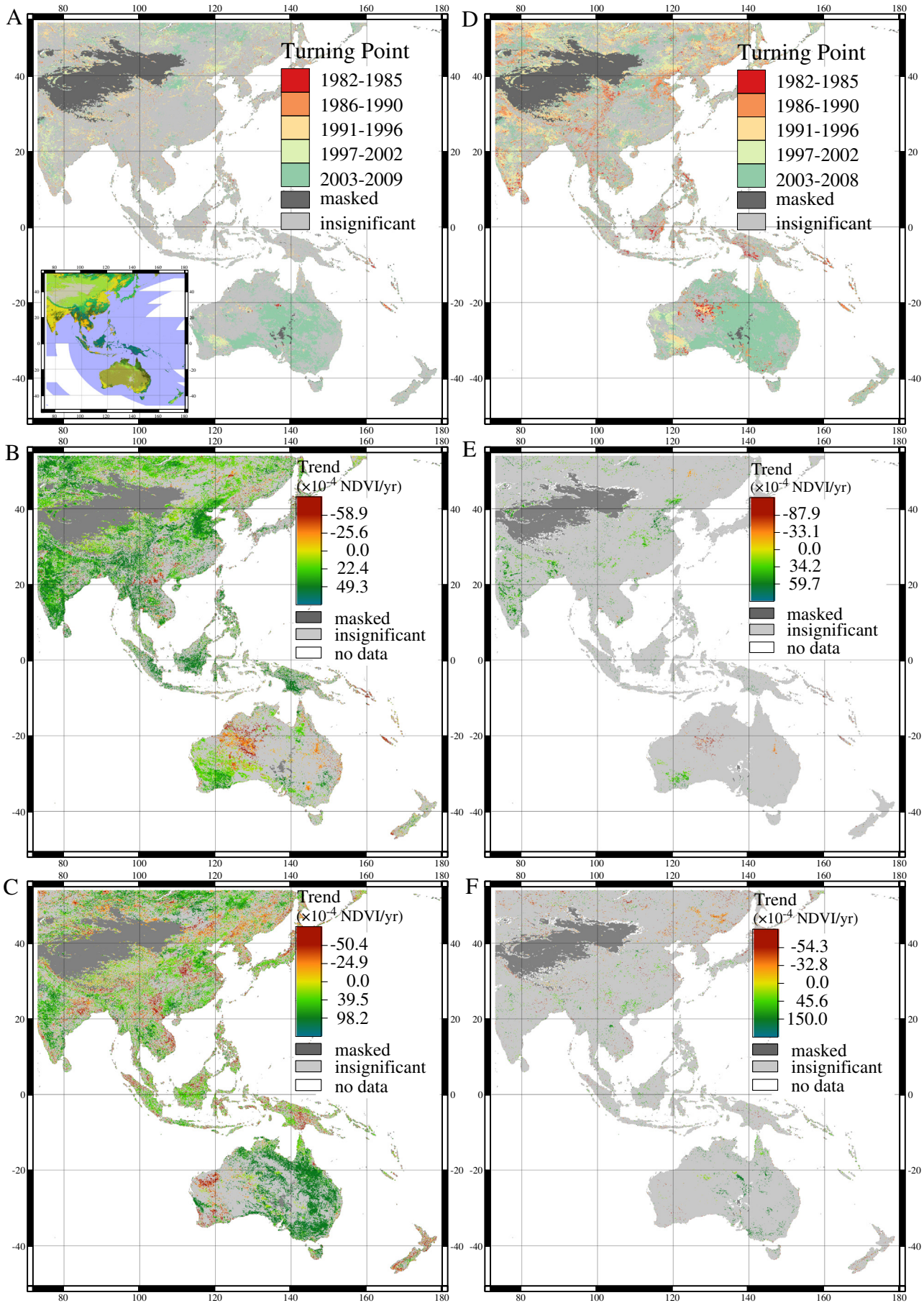
A
Turning Point
1982-1985
1986-1990
1991-1996
1997-2002
2003-2009
masked
insignificant
D
Turning Point
1982-1985
1986-1990
1991-1996
1997-2002
2003-2008
masked
insignificant
B
Trend
(×10-4 NDVI/yr)
-58.9
-25.6
0.0
22.4
49.3
masked
insignificant
no data
E
Trend
(×10-4 NDVI/yr)
-87.9
-33.1
0.0
34.2
59.7
masked
insignificant
no data
C
Trend
(×10-4 NDVI/yr)
-50.4
-24.9
0.0
39.5
98.2
masked
insignificant
no data
F
Trend
(×10-4 NDVI/yr)
-54.3
-32.8
0.0
45.6
150.0
masked
insignificant
no data

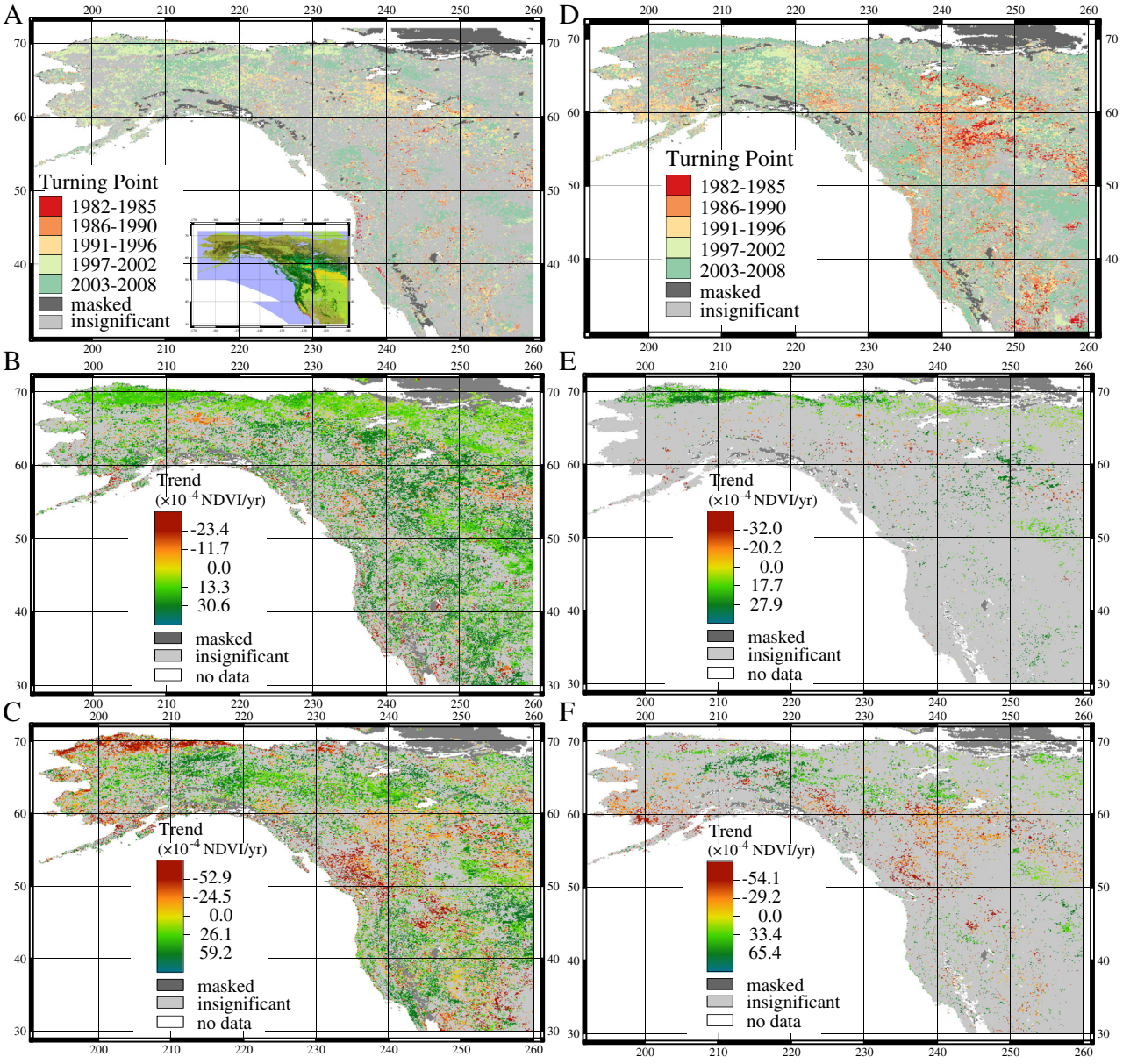

Fig. 6. Same as Fig. 5 but for the North America region.

before 2000, respectively (Fig. 5A, D). The distribution patterns of BP and TP years of annual NDVI trend are similar in the NA (Fig. 6A, D).

4.3.4. Trends of annual NDVI before and after BP and TP

Across the AA subarea, 48% and 46% of the grid cells show statistically significant changes in annual NDVI before and after the BP, respectively (Fig. 5B, C). Of these cells, 82% and 38% display positive NDVI trends before and after the BP, respectively. Before the BP, most of Asia area (~90%) displays positive annual NDVI trends, while majority of Australia area (~66%) shows negative trends (Fig. 5B). After the BP, of these pixels with significant changes in annual NDVI, about 56% show negative trends in Asia and 78% display positive trends in Australia. Whereas both before and after the TP in the AA subregion, only 8% and 6% of the pixels show significant changes in annual NDVI, respectively (Fig. 5E, F). Across the NA subregion, about 56% and 49% of the grid cells show statistically significant changes in annual NDVI before and after the BP, respectively (Fig. 6B, C). Similar to the AA subregion, the majority of these cells displays positive and negative NDVI trends before and after the BP, respectively (Fig. 6B, C). Of the NA subregion, only about 9% displays significantly positive trends in annual NDVI before the TP (Fig. 6E) and about 12% displays significantly trends in annual NDVI after the TP (Fig. 6F), and of these pixels, around half show positive and negative trends in the subregion north and south to 60°N, respectively.

Table 5
The areas ($\times 10^8$ ha) of the pixels where Model 2 and Model 3 respectively determined BPs and TPs of annual NDVI are significantly better than Model 1 using the AIC method ($\Delta\lambda_{1,2} > 2$ or $\Delta\lambda_{1,3} > 2$) during the period of 1982–2011 and their percentages of total land over the Asia–Australia (AA), North America (NA) and the whole Asia–Pacific study regions.

	AA		NA		AP	
	Area	%	Area	%	Area	%
BP	6.86	23.34	4.46	32.87	11.32	26.35
TP	13.44	45.72	7.80	57.46	21.24	49.43

4.3.5. Geographic latitude zone analysis

Trends in NDVI changed differently with respect to latitude. Figs. 7 and 8 show latitudinal zone averaged annual mean and s.d. of NDVI

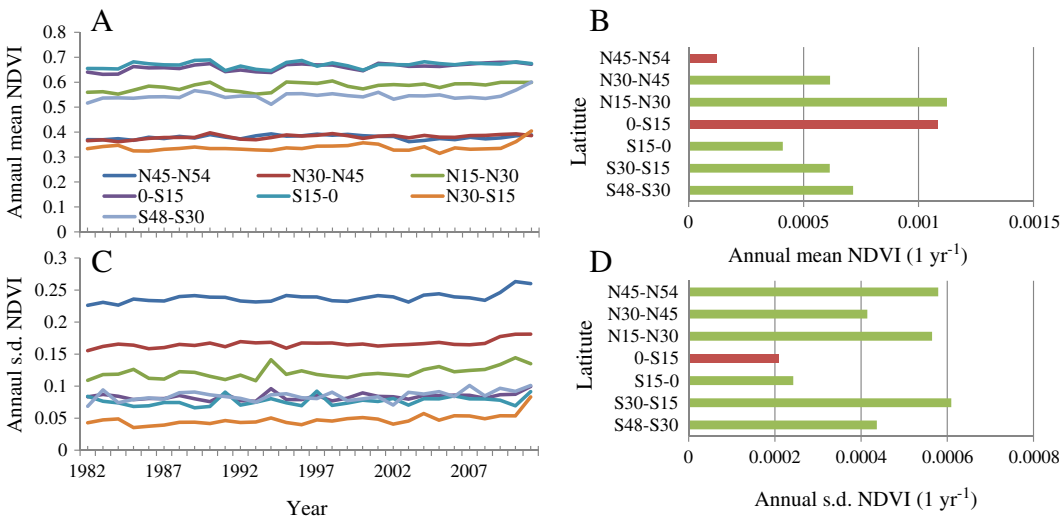

Fig. 7. Changes in vegetation growth dynamics along geographic latitude zones with 15° latitude intervals in the Asia–Australia region from 1982 to 2011. (A) Annual mean NDVI, (B) linear trend in annual mean NDVI; (C) annual standard deviation (s.d.) of NDVI, and (D) linear trend in annual standard deviation (s.d.) of NDVI. In (B) and (D) the green bars indicate the trends are statistically significant ($P < 0.01$), while the insignificant trends are shown in red bars (in (B), zone N45°–54° ($P = 0.48$), zone 0°–S15° ($P = 0.12$) and in (D) zone 0°–15° ($P = 0.10$)). (For interpretation of the references to color in this figure legend, the reader is referred to the web version of this article.)

(panels A and B) and their changes (panels B and D) with 15° intervals from 1982 to 2011 for AA and NA, respectively. Except for the northern mid-latitude band (N45°–54°) and the southern Tropics (0°–S15°), all the zone averaged annual mean NDVI significantly increased at the highest rate of 0.0011 NDVI yr^{-1} in zone N15°–30° from 1982 to 2011 (Fig. 7B). The zonal averaged s.d. of NDVI also significantly increased in AA with higher rates in higher latitudes (Fig. 7D). In NA, the highest latitude zone (N60°–72°, tundra dominated) has the lowest annual mean NDVI values, the highest s.d. values and the highest rate of increase rate in both annual NDVI and standard deviation of NDVI over the past 30 years (Fig. 8).

5. Discussion

5.1. Uncertainties in the data and results

The major source of uncertainties in the detected trends and changes (BPs and TPs) of vegetation photosynthetic activity is from the bias and inter-annual variability of the NDVI time series data. As summarized in Forkel et al. (2013) that the main sources for this inter-annual variability are: (i) insufficient harmonized multi-sensor observations, (ii) weather distortions (e.g. clouds, dust, aerosols or snow cover) and (iii) land surface disturbances (e.g. land cover changes, fire, plant diseases and insect pests) with associated changes in ecosystem structure. As discussed in Section 2.2, the new version GIMMS AVHRR NDVI3g data have overcome the first two problems. Thus only the third source of inter-annual variability would introduce errors in our NDVI time series analyses. In this study, we assume that these errors in our analysis are negligible as the land surface area with obvious disturbances over the last 30 years only accounted for a small proportion compared to non-disturbed area (Sterling & Ducharne, 2008).

The observed dynamics may provide a means to compare against detected trends and changes (BPs and TPs) of vegetation photosynthetic activity in the satellite pixel's spatial location (Tan et al., 2002). At the regional scale and long temporal scale, field-based validation is not feasible because: (i) the GIMMS AVHRR NDVI3g pixel size (~64 km^2) is fairly large. Scaling point field measurements to this coarse resolution would necessarily arise uncertainty from the scaling methodology (Baret et al., 2006), and (ii) the geo-location errors and pixel-shift errors resulting from point spread function would induce uncertainties.

Another source of uncertainty in trend, BP and TP estimations is from the analysis methods, especially from the temporal and spatial aggregations. There are four widely used methods to estimate vegetation photosynthetic activity trends and changes based a long time series of

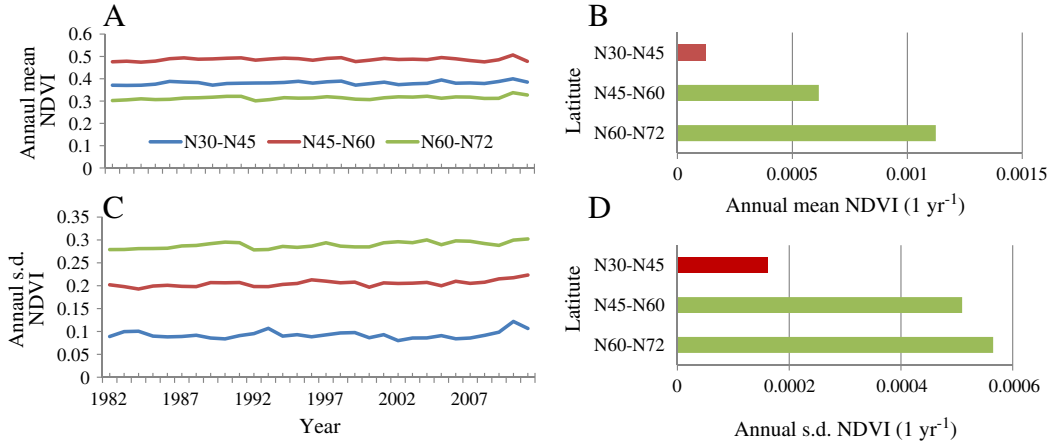

Fig. 8. Same as Fig. 7 but for the North America region. The *P*-value for the insignificant trend in zone N30–N45 (red bars in (B) and in (D)) equal 0.49 and 0.37, respectively. (For interpretation of the references to color in this figure legend, the reader is referred to the web version of this article.)

NDVI data in the literatures, which are (i) estimation on annual aggregated time series (Method AAT, as used in this study) and (ii) estimation based on a season-trend model (Method STM), which is based on the full temporal-resolution NDVI time series to derive the trends and changes using a piecewise linear trend and a seasonal model in a regression relationship (Mann, 1945; Verbesselt et al., 2010); and methods based on de-seasonalized full-resolution time series with removed seasonality to estimate trends (Forkel et al., 2013), which includes two methods: (iii) MAC (mean annual cycle) and (iv) SSA (annual cycle based on singular spectrum analysis).

Forkel et al. (2013) applied all these four trends and changes (BP and TP) estimation methods (AAT, STM, MAC and SSA) to real NDVI time series of Alaska and parts of Yukon to assess differences between methods. They found that Method AAT has usually higher class accuracies as well as a higher total accuracy and Kappa than other methods (Forkel et al., 2013). We also implemented a similar assessment for a spatial subset of the data following the method of Forkel et al. (2013) and found that the analysis based on the annual aggregated values (Method AAT) had the lowest number of wrongly detected BP and TP and the highest accuracy of trend estimation among all the methods. We can therefore expect that the uncertainty in trend and change (BP and TP) estimations in this study is optimally small and the aggregation induced errors and error propagation are minimized.

The regional scale trends of annual mean and annual variance (s.d.) and the BP and TP for the AP, AA and NA regions were estimated using two approaches: (i) aggregated all the pixel NDVI values to form one time series for the individual regions first, and then the regional values were estimated using these three models (see Section 3); and (ii) the NDVI trend and the BP and TP were estimated at the pixel scales based on the 30-year annual mean time series first and then the regional trend was estimated as its average and the BP and TP were estimated as the statistical dominant values over the individual regions. We found the results by these two approaches are identical. This suggests that the spatial aggregation of NDVI would not alter the trend retrieval.

In addition, the period of NDVI time series has a large influence on the detection of linear trends and changes (BPs and TPs). This alerts us to carefully select the length of time series and that the detected trends may change notably following the addition of extra years to the time series (Wessels, Van Den Bergh, & Scholes, 2012). Regarding the BP and TP detection in Methods 2 and 3 (see Sections 3.2 and 3.3), following Piao et al. (2011) and Wang et al. (2011), to avoid error coming from too short segments we only consider segment of the time series with data points larger than 4. A segment with only four data points may be arguably too short to represent sustained ecological change. The exact period of assessment or the minimum acceptable length of time series has a large, but unpredictable influence on the detected trends. Ecosystems may have a rapid change (trend) over a period of 2–5 years and a modest change (trend) over a decadal period or even longer. The validity of the assessment of NDVI time series is compromised and the selection of the minimum acceptable number of data points is a challenge. Researchers should therefore always pay attention to investigate the robustness of the time series data used and make conclusions with a caution.

5.2. Changes in NDVI at the continental scale

We analyzed trends in a time series of vegetation growth dynamics across the Asia–Pacific region over 30 years (1982 through to 2011) using three modes to detect different vegetation dynamic regimes by discerning gradual changes, abrupt changes and changes with a turning point.

The finding of a persistent greening trend over the last 30 years in the AP region is consistent with the results of previous studies based on shorter NDVI data series (e.g., Myneni et al., 1997, 11 years data; Zhou et al., 2001, 18 years data; Nemani et al., 2003, 18 years data; Bunn & Goetz, 2006, 22 years data; Piao et al., 2011, 25 years data; Jong, Verbesselt, Schaepman, & Bruin, 2012, 27 years data). But the linear slope values are different from using the 30-year time series. In general, the averaged slope value was found to decrease with longer time-series of NDVI data. These results are in agreement with previous studies showing recent decreases in vegetation photosynthetic activity in NA and in northern AA (Angert et al., 2005; De Jong, De Bruin, De Wit, Schaepman, & Dent, 2011; Goetz et al., 2005; Lotsch et al., 2005; Park & Sohn, 2010; Piao et al., 2011; Wang et al., 2011). The findings that the increasing rate of NDVI in AA is greater than in NA are consistent with the findings of Zhou et al. (2001).

Overall the AP region persisted in increasing vegetation growth from 1982 to 2011 with an average rate of 5.30×10^{-4} NDVI yr^{-1} and a greening rate for AA of about one time higher than NA (6.22 versus 3.39×10^{-4} NDVI yr^{-1}). This is consistent with most of the previous studies that used different lengths of the NDVI data series (e.g., Bunn & Goetz, 2006; Jong et al., 2012; Myneni et al., 1997; Nemani et al., 2003; Piao et al., 2011; Zhou et al., 2001).

We also compared the trends using annual mean NDVI vs. growing season mean values and found that the identified trends and changes in trends are similar. Piao et al. (2011) reported that in Eurasia the growing season NDVI first significantly increased from 1982 to 1997 and then decreased from 1997 to 2006. Goetz et al. (2005) found that in the boreal NA about one quarter of the forest areas declined in NDVI and that the remainder of the forests showed flat NDVI from 1982 to 2003 with no systematic change in growing season length. More recently it was also reported that in NA and particular in the high latitude regions, a spring vegetation greening trend was evident during the 1980s, which stalled or reversed since the 1990s. Further, summer browning trends occurred in the northwestern region of NA from the early1990s to 2006 (Wang et al., 2011). Unlike most subregions of Eurasia and NA where the increasing trends of growing season NDVI has been reversed or stalled since the late 1990s (Goetz et al., 2005; Piao et al., 2011; Wang et al., 2011), there is no evidence to reject the hypothesis that the overall vegetation activity has kept increasing in both AA and NA within the AP region.

5.3. Spatial patterns of changes in annual NDVI

Our analyses results of the spatial distribution of trends in NDVI during the period 1982–2011 over the NA subregion are consistent with previous studies which found an overall greening trend of North America from 1982 to 1999 (Tucker et al., 2001). The area where the NDVI significantly changed from 1982 to 2011 is much larger than in the study of Goetz et al. (2005) who concluded to be 7.7% of their study area (all of Canada and Alaska) with a significant increases in growing season NDVI (positive trends) and 7.0% with significant decreases (negative trends), considering the period 1982–2003. Our results differ from those of Wang et al. (2011) who showed that most regions of North America, particularly the high latitude regions, had experienced a decrease in summer NDVI considering the period 1982–2006. The findings that the transition from significantly positive to negative NDVI slopes occurred at the boundary between tundra, crop, grasslands and forests (Fig. 3A), is consistent with the findings of Goetz et al. (2005, see Fig. 4 of that paper) using AVHRR-GIMMS data during 1982–2003 and of Beck et al. (2011) considering the period 1982–2008. The fast greening of tundra is likely associated with increasing temperatures and/or growing season length (Goetz et al., 2005). The greening of temperate grasslands/croplands may be related with increasing precipitation and/or irrigation.

Our latitudinal zone analysis reveals that, except for the southern Tropics zonal band (0°–S15°, insignificant changes), all the zonal averaged annual mean and s.d. of NDVI have significant increasing trends and with higher rates in higher latitudes (Fig. 7B, D). This is consistent with the findings by De Jong et al. (2012) that the greening trends were weaker in the Southern Hemisphere (SH) than the NH.

5.4. Trends of annual NDVI before and after BP and TP

The continental-scale BPs identified by Model 2 are 1991, 2003 and 1992 for the AP, AA and NA, respectively. In AA, vegetation productivity increased at a rate of 8.71×10^{-4} NDVI yr^{-1} before the BP year and 29.30×10^{-4} NDVI yr^{-1} after it; in contrast for NA the annual NDVI rapidly increased at a rate of 18.72×10^{-4} NDVI yr^{-1} before the BP year and after the BP it dropped down to 3.96×10^{-4} NDVI yr^{-1}. Model 3 detected TPs are 2008, 1987 and 2008 for the AA, NA and AP, respectively. In the AA subregion the vegetation greening rate is an order larger after 2008 (TP) than before it (58.04 versus 4.23×10^{-4} NDVI yr^{-1}). By contrast in NA the annual productivity increased very quickly from 1982 to 1987 and then almost stalled after the TP (23.03 versus 1.50×10^{-4} NDVI yr^{-1}) and up until 2011. This is different from the findings of Piao et al. (2011) that in Eurasia the growing season NDVI first significantly increased from 1982 to 1997 and then decreased from 1997 to 2006. The trends calculated by these three approaches (Eqs. 1–3) are positive from 1982 through to 2011 for most months, particularly for growing season months whereas the detected significant BPs and TPs vary month to month with a broad range of occurrence from the 1980s to recent years. The trends before and after BP are statistically significant for most of months over the entire AP. However trends are rarely significantly different before and after TP, suggesting that the models 1 and 2 are a better fit to the 30 years of time series satellite observations. However, NDVI changes in most growing season months are better described by Model 3 than Model 1. Many previous studies have found that there was a significant change in the trends of NDVI around the 1990s, the detected BP in this study is different from previous studies using different lengths of time series data. For instance, Piao et al. (2011) found that 1997 was the turning point over the 25 years (1982–2006) in Eurasia. We can conclude that the BP varies with regions and the lengths of time series of data used.

5.5. Drivers of changes in vegetation photosynthetic activity dynamics

Global climatic changes over the past 30 years have altered (mainly enhanced but also constrained in part) plant growth (Nemani et al., 2003; Zhao & Running, 2010). The mechanisms behind the temporal and spatial dynamics of vegetation productivity in the context of accelerated global environmental change are not well understood. The results presented in this study demonstrate that vegetation productivity and variance (seasonality) in the AP vary among different subregions. There are different spatial patterns for abrupt, turning and gradual changes with dramatic variations in BPs and TPs, indicating complexity in vegetation growth dynamics and a nonlinear response of vegetation to global climatic changes and other drivers. The significant BPs and TPs concentrated in the region of Guansu–Ningxia–Shanxi–Hubei–Jiangxi provinces, for instance, are very likely to be associated with human activities, because these BPs and TPs occurring from 2000 located at the central well-implemented area of China's "grain to green" project started from 2000. Divergence between the findings and those of previous researchers using different lengths of NDVI data series at different scales, suggests that continuing efforts to monitor vegetation changes (in situ and satellite observations) over time and at broad scales are greatly needed and critical for the management of ecosystems, biodiversity, and for diagnosing and adapting to global climatic changes. Previous studies suggest that multiple mechanisms have changed vegetation dynamics, including climatic factors (temperature, drought stress), climate change induced disturbance (fire, plant diseases and insect pests), and human activity induced environmental changes (e.g., land use land cover change, forest regrowth, nitrogen deposition, CO_2 fertilization, ozone pollution and aerosols). Moving forward it is difficult to understand vegetation dynamics and its interaction with global climatic change. It is likewise difficult to well predict future vegetation growth and carbon sinks, without linking of these observations to mechanistic terrestrial ecosystem processes models which integrate all the satellite and in situ observations.

We also implemented an explicit geospatial analysis to improve our understanding of physiological mechanisms by which temperature and precipitation affect plant growth, which will be reported in a companion paper (entitled changes in terrestrial photosynthetic activity trends across the Asia–Pacific region associated with land cover and climate from 1982 to2011). About 40% of the AA subregion has significant correlations between annual mean NDVI anomalies and annual mean temperature anomalies (21% positive, and most of which distributes in South and East Asia; and 18% negative and mostly distributes in Australia). The pixels with significantly positive and negative correlations between annual mean NDVI anomalies and annual total precipitation anomalies respectively account for 32% and 9% of the AA subregion. Above 90% of Australia displays positive correlation and majority of the AA north to N50° displays negative correlation. Of the NA region, the pixels where annual mean NDVI anomalies positively and negatively correlated with annual mean temperature anomalies respectively account for 34% and 4%, while only 26% has significant correlations between annual mean NDVI anomalies and annual total precipitation anomalies (15% positive and 11% negative).

Numerous studies have documented that interdecadal climate change is driven by natural interdecadal variability as well as anthropogenic forcing, especially at the regional (continental/basin) scale (Liu, 2012). The interdecadal variations in climate over the AP region are predominately impacted by the Pacific Decadal Oscillation (Mills & John, 2013), which is described as a long-lived El Niño-like pattern of Pacific climate variability (Zhang, Wallace, & Battisti, 1997). The overall correlation between annual mean NDVI and PDO was found to be statistically negative in the AP region ($R = -0.41$, $P = 0.02$) and is more pronounced in the AA subregion ($R = -0.47$, $P = 0.008$) and insignificant in the NA region ($R = -0.11$, $P = 0.57$).

Acknowledgments

This research was supported by research grants (2010CB950902 and 2010CB9504) under the Global Change Program of the Chinese Ministry of Science and Technology, a research grant named "Adaptation of Asia–Pacific Forests to Climate Change" (project #APFNet/2010/PPF/001) founded by the Asia–Pacific Network for Sustainable Forest Management and Rehabilitation, a research grant (2012ZD010) of the Key Project for the Strategic Science Plan in IGSNRR, CAS, the research grants (41071059 & 41271116) funded by the National Science Foundation of China, a Research Plan of LREIS (O88RA900KA), CAS, and "One Hundred Talents" program funded by the Chinese Academy of Sciences. We thank Dr. C.J. Tucker and Dr. J. Pinzon of NASA GSFC for making available the GIMMS NDVI3g data set.

References

Anderson, R. G., Canadell, J. G., Randerson, J. T., Jackson, R. B., Hungate, B. A., Baldocchi, D. D., et al. (2010). Biophysical considerations in forestry for climate protection. *Frontiers in Ecology and the Environment*, *9*, 174–182.

Angert, A., Biraud, S., Bonfils, C., et al. (2005). Drier summers cancel out the CO_2 uptake enhancement induced by warmer springs. *Proceedings of the National Academy of Sciences of the United States of America*, *102*, 10823–10827.

Bai, J., & Perron, P. (2003). Computation and analysis of multiple structural change models. *Journal of Applied Econometrics*, *18*, 1–22.

Baret, F., Morissette, J. T., Fernandes, R. A., Champeaux, J. L., Myneni, R. B., Chen, J., et al. (2006). Evaluation of the representativeness of networks of sites for the global validation and intercomparison of land biophysical products: Proposition of the CEOS-BELMANIP. *IEEE Transactions on Geoscience and Remote Sensing*, *44*, 1794–1803.

Beck, H. E., McVicar, T. R., van Dijk, A. I. J. M., Schellekens, J., de Jeu, R. A.M., & Bruijnzeel, L. A. (2011). Global evaluation of four AVHRR–NDVI data sets: Intercomparison and assessment against Landsat imagery. *Remote Sensing of Environment*, *115*, 2547–2563.

Box, E. O., Holben, B. N., & Kalb, V. (1989). Accuracy of the AVHRR vegetation index as a predictor of biomass, primary productivity and net CO_2 flux. *Plant Ecology*, *80*, 71–89.

Bunn, A., & Goetz, S. F. (2006). *Trends in satellite-observed circumpolar photosynthetic activity from 1982 to 2003: The influence of seasonality, cover type, and vegetation density.* Earth Interactions, 16.

Burnham, K. P., & Anderson, D. R. (2002). *Model selection and multimodel inference: A practical information-theoretic approach*. Berlin: Springer.

Catrin, M. M., & John, E. W. (2013). Seasonal variation and spatial patterns of the atmospheric component of the Pacific Decadal Oscillation. *Journal of Climate*, *26*, 1575–1594.

Congalton, R. G. (1991). A review of assessing the accuracy of classifications of remotely sensed data. *Remote Sensing of Environment*, *37*, 35–46.

Cruz, R. V., Harasawa, H., Lal, M., et al. (2007). Asia, in climate change 2007: Impacts, adaptation and vulnerability. In M. L. Parry (Ed.), *Contribution of working group II to the fourth assessment report of the intergovernmental panel on climate change* (pp. 469–506). Cambridge, U.K.: Cambridge Univ. Press.

De Jong, R., De Bruin, S., De Wit, A., Schaepman, M. E., & Dent, D. L. (2011). Analysis of monotonic greening and browning trends from global NDVI time-series. *Remote Sensing of Environment*, *115*, 692–702.

De Jong, R., Verbesselt, J., Schaepman, M. E., & de Bruin, S. (2012). Trend changes in global greening and browning: Contribution of short-term trends to longer-term change. *Global Change Biology*, *18*, 642–655.

De Jong, R., Verbesselt, J., Zeileis, A., & Schaepman, M. E. (2013). Shifts in global vegetation activity trends. *Remote Sensing*, *5*, 1118–1133.

Defries, R. S., & Townshend, J. R. G. (1994). NDVI-derived land-cover classifications at a global-scale. *International Journal of Remote Sensing*, *15*, 3567–3586.

Donohue, R. J., Mcvicar, T. R., & Roderick, M. L. (2009). Climate-related trends in Australian vegetation cover as inferred from satellite observations, 1981–2006. *Global Change Biology*, *15*, 1025–1039.

Fensholt, R., & Proud, S. R. (2012). Evaluation of earth observation based global long term vegetation trends—Comparing GIMMS and MODIS global NDVI time series. *Remote Sensing of Environment*, *119*, 131–147.

Fensholt, R., Rasmussen, K., Nielsen, T. T., & Mbow, C. (2009). Evaluation of earth observation based long term vegetation trends — Intercomparing NDVI time series trend analysis consistency of Sahel from AVHRR GIMMS, Terra MODIS and SPOT VGT data. *Remote Sensing of Environment*, *113*, 1242–1255.

Forkel, M., Carvalhais, N., Verbesselt, J., Mahecha, M.D., Neigh, C. S. R., & Reichstein, M. (2013). Trend change detection in NDVI time series: Effects of inter-annual variability and methodology. *Remote Sensing*, *5*, 2113–2144.

Francesco Ficetola, G., & Denoël, M. (2009). Ecological thresholds: An assessment of methods to identify abrupt changes in species—habitat relationships. *Ecography*, *32*, 1075–1084.

Goetz, S. J., Bunn, A. G., Fiske, G. J., & Houghton, R. A. (2005). Satellite-observed photosynthetic trends across boreal North America associated with climate and fire disturbance. *Proceedings of the National Academy of Sciences of the United States of America*, *102*, 13521–13525.

Goetz, S., & Prince, S. D. (1999). Modelling terrestrial carbon exchange and storage: Evidence and implications of functional convergence in light-use efficiency. *Advances in Ecological Research*, *28*, 57–92.

Goward, S. N., Tucker, C. J., & Dye, D.G. (1985). North American vegetation patterns observed with theNOAA-7 advanced very high resolution radiometer. *Plant Ecology*, *64*, 3–14.

Hansen, J., Ruedy, R., Sato, M., & Lo, K. (2010). Global surface temperature change. *Reviews of Geophysics*, *48*(RG4004), 4001–4029.

Høgda, K. A., Tømmervik, H., & Karlsen, S. R. (2013). Trends in the start of the growing season in Fennoscandia 1982–2011. *Remote Sensing*, *5*, 24304–24318.

Jackson, R. B., Randerson, J. T., Canadell, J. G., et al. (2008). Protecting climate with forests. *Environmental Research Letters*, *3*, 044006.

Jong, R., Verbesselt, J., Schaepman, M. E., & Bruin, S. (2012). Trend changes in global greening and browning: Contribution of short-term trends to longer-term change. *Global Change Biology*, *18*, 642–655.

Latif, M., & Barnett, T. P. (1994). Causes of decadal climate variability over the north Pacific and North America. *Science*, *266*, 634–637.

Liu, Z. (2012). Dynamics of interdecadal climate variability: A historical perspective. *Journal o\f Climate*, *25*, 1963–1995.

Lotsch, A., Friedl, M.A., Anderson, B. T., & Tucker, C. J. (2005). Response of terrestrial ecosystems to recent Northern Hemispheric drought. *Geophysical Research Letters*, *32*, L06705.

Mann, H. B. (1945). Nonparametric tests against trend. *Econometrica*, *13*, 245–259.

Miao, C., Yang, L., Chen, X., & Gao, Y. (2012). The vegetation cover dynamics (1982–2006) in different erosion regions of the Yellow River Basin, China. *Land Degradation & Development*, *23*, 62–71.

Mills, C. M., & John, E. W. (2013). Seasonal variation and spatial patterns of the atmospheric component of the Pacific Decadal Oscillation. *Journal of Climate*, *26*, 1575–1594.

Myneni, R. B., Hall, F. G., Sellers, P. J., & Marshak, A. L. (1995). The interpretation of spectral vegetation indexes. *Geoscience and Remote Sensing, IEEE Transactions on*, *33*, 481–486.

Myneni, R. B., Keeling, C., Tucker, C., Asrar, G., & Nemani, R. (1997). Increased plant growth in the northern high latitudes from 1981 to 1991. *Nature*, *386*, 698–702.

Nemani, R. R., Keeling, C. D., Hashimoto, H., Jolly, W. M., Piper, S.C., Tucker, C. J., et al. (2003). Climate-driven increases in global terrestrial net primary production from 1982 to 1999. *Science*, *300*, 1560–1563.

Newman, M., Gilbert, P. C., & Michael, A. A. (2003). Enso-forced variability of the Pacific Decadal Oscillation. *Journal of Climate*, *16*, 3853–3857.

Olsson, L., Eklundh, L., & Ardo, J. (2005). A recent greening of the Sahel — Trends, patterns and potential causes. *Journal of Arid Environments*, *63*, 556–566.

Park, H. S., & Sohn, B. J. (2010). Recent trends in changes of vegetation over East Asia coupled with temperature and rainfall variations. *Journal of Geophysical Research*, *115*, D14101.

Patterson, R. T., Chang, A. S., Prokoph, A., Roe, H. M., & Swindles, G. T. (2013). Influence of the Pacific Decadal Oscillation, El Niño-Southern Oscillation and solar forcing on climate and primary productivity changes in the northeast Pacific. *Quaternary Internation*, 1–16.

Peng, S., Chen, A., Xu, L., Cao, C., Fang, J., Myneni, R. B., et al. (2011). Recent change of vegetation growth trend in China. *Environmental Research Letters*, *6*, 044027.

Peng, J., Liu, Z., Liu, Y., Wu, J., & Han, Y. (2012). Trend analysis of vegetation dynamics in Qinghai–Tibet Plateau using Hurst Exponent. *Ecological Indicators*, *14*, 28–39.

Piao, S. L., Fang, J. Y., Zhou, L. M., et al. (2003). Interannual variations of monthly and seasonal normalized difference vegetation index (NDVI) in China from 1982 to 1999. *Journal of Geophysical Research*, *108*(D14), 4401. http://dx.doi.org/10.1029/2002JD002848 (2003).

Piao, S., Wang, X., Ciais, P., Zhu, B., Wang, T., & Liu, J. (2011). Changes in satellite-derived vegetation growth trend in temperate and boreal Eurasia from 1982 to 2006. *Global Change Biology*, *17*, 3228–3239.

Preston, B.L., Suppiah, R., Macadam, I., & Bathols, J. (2006). *Climate change in the Asia/Pacific region: A consultancy report prepared for the climate change and development roundtable*. Melbourne: Climate Change Impacts and Risk, CSIRO Marine and Atmospheric Research (October, 89 pp.).

Rouse, J. W., Haas, R. H., Schell, J. A., & Deering, D. W. (1973). Monitoring vegetation systems in the Great Plains with ERTS. *NASA Third Earth Resources Technology Satellite (ERTS) symposium* (Washington DC, USA).

Scheffer, M., Carpenter, S., Foley, J. A., Folke, C., & Walker, B. (2001). Catastrophic shifts in ecosystems. *Nature*, *413*, 591–596.

Slayback, D. A., Pinzon, J. E., Los, S. O., & Tucker, C. J. (2003). Northern hemisphere photosynthetic trends 1982–99. *Global Change Biology*, *9*, 1–15.

Sterling, S., & Ducharne, A. (2008). Comprehensive data set of global land cover change for land surface model applications. *Global Biogeochemical Cycles*, *22*, GB3017. http://dx.doi.org/10.1029/2007GB002959.

Sun, J., Wang, X., Chen, A., Ma, Y., Cui, M., & Piao, S. (2011). NDVI indicated characteristics of vegetation cover change in China's metropolises over the last three decades. *Environmental Monitoring and Assessment*, *179*, 1–14.

Swift, T. L., & Hannon, S. J. (2010). Critical thresholds associated with habitat loss: A review of the concepts, evidence, and applications. *Biological Reviews*, *85*, 35–53.

Tan, B., Woodcock, C. E., Hu, J., Zhang, P., Ozdogan, M., Huang, D., et al. (2002). The impact of gridding artifacts on the local spatial properties of MODIS data: Implications for validation, compositing, and band-to-band registration across resolutions. *Remote Sensing of Environment*, *83*, 195–213.

Toms, J.D., & Lesperance, M. L. (2003). Piecewise regression: A tool for identifying ecological thresholds. *Ecology*, *84*, 2034–2041.

Tucker, C. J. (1979). Red and photographic infrared linear combinations for monitoring vegetation. *Remote Sensing of Environment*, *8*, 27–150.

Tucker, C. J., Pinzon, J. E., Brown, M. E., Slayback, D. A., Pak, E. W., Mahoney, R., et al. (2005). An extended AVHRR 8-km NDVI dataset compatible with MODIS and SPOT vegetation NDVI data. *International Journal of Remote Sensing*, *26*, 4485–4498.

Tucker, C. J., Slayback, D. A., Pinzon, J. E., Los, S. O., Myneni, R. B., & Taylor, M. G. (2001). Higher northern latitude normalized difference vegetation index and growing season trends from 1982 to 1999. *International Journal of Biometeorology*, *45*, 184–190.

USAID United States Agency for International Development (2010). *Asia–Pacific regional climate change adaptation assessment*. Final report: Findings and recommendations. Connecticut, NW: International Resources Group (145 pp.).

Verbesselt, J., Hyndman, R., Newnham, G., & Culvenor, D. (2010). Detecting trend and seasonal changes in satellite image time series. *Remote Sensing of Environment*, *114*, 106–115.

Wang, X., Piao, S., Ciais, P., Li, J., Friedlingstein, P., Koven, C., et al. (2011). Spring temperature change and its implication in the change of vegetation growth in North America from 1982 to 2006. *Proceedings of the National Academy of Sciences*, *108*, 1240–1245.

Wang, S. P., Wang, Z. H., Piao, S. L., & Fang, J. Y. (2010). Regional differences in the timing of recent air warming during the past four decades in China. *Chinese Science Bulletin*, *55*, 1968–1973.

Wessels, K. J., Van Den Bergh, F., & Scholes, R. J. (2012). Limits to detectability of land degradation by trend analysis of vegetation index data. *Remote Sensing of Environment*, *125*, 10–22.

Xu, L., Myneni, R. B., Chapin, F. S. I. I. I., Callaghan, T. V., Pinzon, J. E., Tucker, C. J., et al. (2013). Temperature and vegetation seasonality diminishment over northern lands. *Nature Clim. Change*. http://dx.doi.org/10.1038/nclimate1836.

Yao, C., Yang, S., Qian, W., Lin, Z., & Wen, M. (2008). Regional summer precipitation events in Asia and their changes in the past decades. *Journal of Geophysical Research*, *113*, D17107. http://dx.doi.org/10.1029/2007JD009603.

Zeileis, A., Kleiber, C., Krämer, W., & Hornik, K. (2003). Testing and dating of structural changes in practice. *Computat. Statist. Data Anal.*, *44*, 109–123.

Zeng, F. W., Collatz, G. J., Pinzon, J. E., & Ivanoff, A. (2013). Evaluating and quantifying the climate-driven interannual variability in Global Inventory Modeling and Mapping Studies (GIMMS) Normalized Difference Vegetation Index (NDVI3g) at global scales. *Remote Sensing*, *5*, 3918–3950.

Zhang, Y., Wallace, J. M., & Battisti, D. (1997). ENSO-like interdecadal variability: 1900–93. *Journal of Climate*, *10*, 1004–1020.

Zhao, M., & Running, S. W. (2010). Drought-induced reduction in global terrestrial net primary production from 2000 through 2009. *Science*, *329*, 940–943.

Zhou, L., Tucker, C. J., Kaufmann, R. K., Slayback, D. A., Shabanov, N. V., & Myneni, R. (2001). Variations in northern vegetation activity inferred from satellite data of vegetation index during 1981 to 1999. *Journal of Geophysical Research*, *106* (20,069–20,083).